Novel Moving Average Filter for Detecting rms Voltage Step Changes in Triggerless PQ Data

Alvaro Furlani Bastos, *Student Member, IEEE,* Keng-Weng Lao, *Member, IEEE,*
Grazia Todeschini, *Senior Member, IEEE,* and Surya Santoso, *Fellow, IEEE*

***Abstract*—The voluminous amount of raw waveform data recorded by triggerless power quality monitors contain conspicuous and inconspicuous disturbance events. Data reduction and detection techniques are needed to efficiently extract useful information hidden in the raw data and identify power quality disturbances. The overall objective of this study is to use step changes in the rms voltage profile as an alternative triggering feature for automatically detecting switching events. The full characterization of the event is based on processing a small portion of the voltage waveform selected around the detected rms voltage step change. A filtering method is proposed to smooth out rapid fluctuations in the rms voltage profile during steady-state operation, while preserving the sharp edges caused by rms voltage step changes. Once the rms voltage profile has been filtered, adaptive limits based on the median absolute deviation are computed for detecting rms voltage step changes. The effectiveness of the proposed technique is evaluated using triggerless voltage waveforms to detect capacitor switching events. The use of the filtered rms voltage profile allows accurate detection of capacitor energizing and de-energizing events, while more than 50% of the detections in the unfiltered profile correspond to false-positives.**

***Index Terms*—capacitor switching, power quality, moving average and median filters, rms voltage profile, triggerless data, voltage step change**

I. Introduction

POWER quality monitors traditionally employ specific triggering features to detect disturbances and store them as individual events. The disturbances are often recorded as instantaneous voltage and current waveforms, a few cycles preceding and following the trigger time. A recent trend in power quality monitoring shows a growing interest in triggerless continuous measurements of instantaneous voltage and current waveforms. This approach allows capturing all possible disturbance events, even if they are not accompanied by conspicuous transients [1]. However, such method inevitably results in voluminous amount of data [2], [3]. Novel triggering methods are necessary to parse through the voluminous data and detect conspicuous and inconspicuous disturbance events.

A. F. Bastos is with the Department of Electrical and Computer Engineering, The University of Texas at Austin, USA, and also with the CAPES Foundation within the Ministry of Education, Brazil (e-mail: alvaro.fbastos@utexas.edu).

K.-W. Lao is with the Department of Electrical and Computer Engineering, University of Macau, Macao, China, and also with the Department of Electrical and Computer Engineering, The University of Texas at Austin, USA (e-mail: johnnylao@umac.mo).

G. Todeschini is with the College of Engineering, Swansea University, Swansea, UK (e-mail: grazia.todeschini@swansea.ac.uk).

S. Santoso is with the Department of Electrical and Computer Engineering, The University of Texas at Austin, USA (e-mail: ssantoso@mail.utexas.edu).

Well-known methods such as wavelet transform and comparison of consecutive cycles of data are efficient tools in detecting conspicuous disturbances in the instantaneous voltage and current waveforms [4]. On the other hand, these methods are not suitable for triggerless data, due to their inability to detect inconspicuous disturbances. For example, capacitor energizing operations can be identified by the transient in voltage and current waveforms, while the transient-free de-energizing operations must be identified through a step change in the rms voltage profile [5]. Other events that cause an rms voltage step change and may present little to no transients are, for example, transformer tap-changing, voltage regulator operation, and switching of large loads [6].

IEC and IEEE standards establish that the rms voltage values should be computed over one-cycle sliding window, and updated every half-cycle, denoted as $U_{rms(1/2)}$ [7], [8]. In 2015, IEC released recommendations for detection and characterization of voltage variation events that do not belong to the sag/swell categories due to their small voltage magnitude variation (below 10%), including the rms voltage step changes mentioned previously. It established that a transition in rms voltage between two steady-state conditions occurs when the difference between the latest computed $U_{rms(1/2)}$ value and a reference voltage exceeds a variable threshold. This threshold is defined as a percentage of the arithmetic mean of the $U_{rms(1/2)}$ values computed during the previous 1 second (120 rms values for a 60 Hz system). The standard recommends a threshold between 1% and 6%, and this value is set by the user according to the desired application. This recommendation cannot be generalized to detect a wide variety of events, as the magnitude of the rms voltage step change may be lower than 1%. For example, voltage regulators commonly provide a range from -10% to +10% with 32 steps, each step representing a 0.625% variation in the voltage level [9]. Another example is the steady-state voltage variation caused by switching a capacitor bank, which is usually in the range 0.36% - 4% at the capacitor terminals, and decreases at points further upstream the bank location [10].

Since the events mentioned above cannot be identified by applying the methods used for conspicuous disturbances, and the corresponding rms voltage variations are usually lower than the threshold for sag/swell detection, this paper proposes an event detection technique adopting the rms voltage step change as an alternative triggering feature. The definition of $U_{rms(1/2)}$ results in a non-smooth rms voltage profile, as the loads vary intermittently between consecutive rms voltage computations [6]. The presence of high levels of fluctuation

in the rms voltage profile hinders the detection of rms voltage step changes, possibly affecting the performance of algorithms developed for identification of power quality disturbances. Therefore, prior to being used in the disturbances identification process, the rms voltage profile must be processed to remove the rapid voltage fluctuations. The desired output of this process is an rms voltage profile with high signal-to-noise ratio and sharp edges during the step changes.

Filtering the input signal through a moving average filter is a simple and easily implementable approach to remove the rapid rms voltage fluctuations. This low pass filter removes the noise component from the data by averaging M samples (the filter length) to produce a single output value. Although the smoothness of the output signal increases with M, the sharp edges become blunt; therefore, this approach is unfit for detecting switching events [11], [12]. Increasing beyond one-cycle the length of the sliding window used to compute the rms voltage profile results in a similar smoothing effect [6].

Another approach consists in applying a median filter, which removes impulsive noise while preserving sharp edges and trends. However, an unsuitable choice of the filter length may result in the output signal undesirably following the rapid voltage fluctuations [13], [14]. As voltage fluctuation happens randomly in the system, there is no straightforward way to optimize the length of the median filter.

Given the limitations discussed above, the goal of this paper is to: (a) propose a novel filter to attenuate the rapid fluctuations observed in rms voltage profiles, while preserving the sharp edges during rms voltage step changes; and (b) develop a technique to automatically detect these rms voltage step changes, which can be applied to triggerless power quality measurement data to detect all rms voltage variations. Its main contribution is the ability to detect not only conspicuous, but also inconspicuous disturbances. RMS voltage profile computation and inconspicuous disturbances caused by capacitor de-energizing operations are described in Section II. Removal of the rapid voltage fluctuations in the rms voltage profile is performed by a novel digital filter as discussed in Section III. Additionally, an approach to compute adaptive limits for automatic detection of rms voltage step changes is presented. Rather than setting a hard threshold for the minimum variation in voltage between two steady-state conditions, these adaptive limits are based on statistical tests and rms values computed prior to the current instant. Finally, a data reduction technique is described: portions of the voltage and current waveforms without a detected rms voltage step change do not represent a switching event; therefore, they can be disregarded from detailed analysis, reducing the time and computational effort required to identify and characterize switching events. The proposed technique is applied to the analysis of triggerless voltage field data, and the results are discussed in Section IV.

II. Problem Description

A. Instantaneous Voltage and rms Profile Models

The instantaneous voltage in power systems is commonly composed of fundamental and harmonic frequency components, and, less frequently, a dc offset. The sampled phase voltage, $v[n]$, can be modeled as the sum of time-varying sinusoids and superimposed noise, as represented in (1).

$$v[n] = \sum_{m=0}^{H} V_m[n] \sin\left(\omega_m n + \phi_m[n]\right) + d[n] \qquad (1)$$

where V_m, ω_m, and ϕ_m are the magnitude, angular frequency, and phase angle of the m^{th} harmonic, respectively, and $d[n]$ denotes superimposed noise. The choice of the highest harmonic order H depends on the event under analysis; a frequently adopted value is 50 [15]. The noise $d[n]$ is introduced by interference in the measuring device. Note that this model also describes short-duration and high-frequency transient events, as the magnitudes V_m of the corresponding high order components increase during the event.

The voltage magnitude V_m can be decomposed into four terms: steady-state nominal voltage provided by the generators (V_m^{nom}), slow and fast variations caused by fluctuations in the aggregate load connected to the system (V_m^{slow} and V_m^{fast}, respectively), and step change component caused by capacitor switching, voltage regulator operations, or connection/disconnection of large loads (V_m^{step}). Not all components are present simultaneously; for example, V_m^{step} is non-zero only during voltage step change events.

The rms voltage value at instant k is computed from the instantaneous voltage values over a one-cycle long sliding window and updated every half cycle [7], [8]:

$$V_{rms}[k] = \sqrt{\frac{1}{N} \sum_{p=k-N+1}^{k} v[p]^2} \qquad (2)$$

where N is the number of samples per cycle. The rms voltage profile can be divided into components equivalent to each term of V_m (V_{rms}^{nom}, V_{rms}^{slow}, V_{rms}^{fast}, V_{rms}^{step}) and superimposed noise (d_{rms}). The term d_{rms} includes two components: noise introduced by the measuring device, and non-integer number of cycles within the sliding window for rms computation. The latter is due to the non-synchronization of the fixed sampling frequency to the varying power frequency [8].

The goal of this paper is to develop a technique to detect rms voltage step changes, i.e., instants at which V_{rms}^{step} is non-zero. Since rms voltage step changes correspond to fast variations in the system voltage level, V_{rms}^{step} occurs at the same time scale as V_{rms}^{fast} and d_{rms}. Therefore, these two components must be attenuated to obtain a robust algorithm for detection of non-zero V_m^{step}. V_{rms}^{slow} does not affect the detection of rms voltage step changes due to its slow-varying characteristic.

B. Capacitor Switching Operation

Capacitor banks switching causes one of the most common rms voltage step change observed in transmission and distribution systems. Capacitor banks provide voltage support under heavy load conditions, instantaneously increasing the system steady-state voltage after they are energized.

Capacitor energizing operations are accompanied by transients in voltage and current waveforms. Such behavior is caused by the interaction between the bank capacitance and the power system inductance. The voltage is initially pulled toward

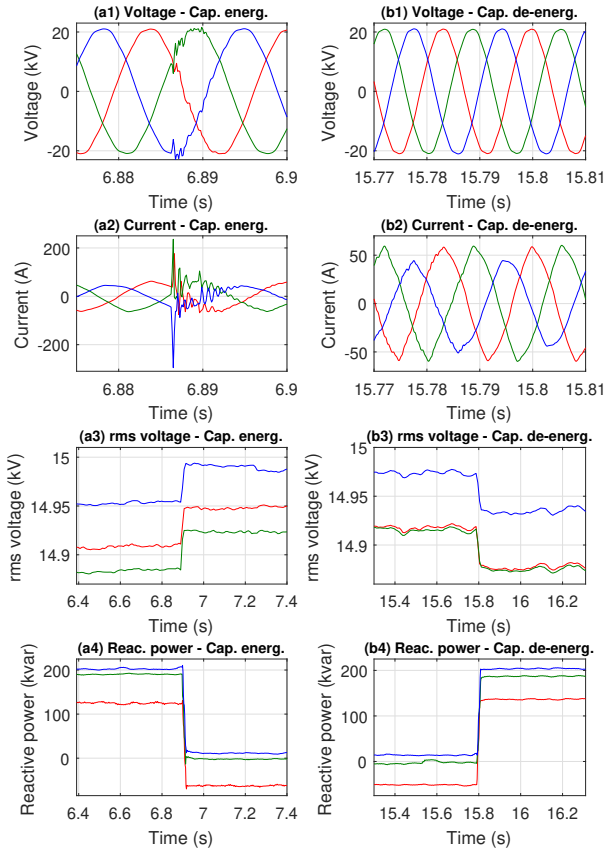

Fig. 1. Typical voltage and current waveforms, rms voltage profile, and reactive power flow during capacitor (a1-a4) energizing and (b1-b4) de-energizing operations.

zero and oscillates at the system natural frequency (usually between 300 Hz and 1000 Hz). This transient typically lasts for 0.25-0.5 cycle, during which the voltage usually overshoots between 1.0 and 1.4 pu, depending on the system damping [16]. The reactive power support provided by the capacitor bank is translated into a reduction of reactive power flow between the source and the capacitor bank location.

On the other hand, normal de-energizing operations do not result in any voltage or current transient oscillations. These events are characterized by the reduction of system voltage and reactive power support (the latter is applicable only to banks located downstream from the monitoring location) [5].

Typical voltage and current waveforms, rms voltage profile, and reactive power flow during capacitor energizing and de-energizing operations are represented in Fig. 1.

The transients observed during a capacitor energizing operation can be used as signatures for identifying and characterizing these events through a discrete wavelet transform (DWT) [5]. Although this method is very robust and accurate, it requires significant computational effort, as the DWT of the voltage signal must be computed continuously. Additionally, this method is not applicable to detect capacitor de-energizing operations due to the absence of transients.

A step change in rms voltage is the only parameter common to all capacitor switching operations. The technique proposed in this paper enables an efficient and robust detection of steady-state rms voltage variation during capacitor switching events, including the transient-free de-energizing operations. This process assists in the identification of capacitor switching events by selecting a smaller portion of the voltage and current waveforms. Applying the DWT to the selected data – rather than to the continuously sampled voltage – significantly reduces the computational effort required to identify and characterize these events. Although the proposed methodology is illustrated in relation to capacitor switching, it is applicable to the identification of any events that create an rms voltage step change.

III. Methodology

This section presents the algorithm developed for filtering the rms voltage profile. The filter input consists of the rms voltage profile computed as in (2), and stored in the vector V_{input}, while the output filtered rms voltage profile is stored in V_{rms}^{filt}. The filtering process is performed by sliding a w-samples (filter length) long window through the entire input signal. The filtered output at index k is computed using rms voltage values at indices ranging from $k-\lfloor w/2 \rfloor$ to $k+\lfloor w/2 \rfloor$, where $\lfloor . \rfloor$ denotes the floor function. The sliding window is defined as (3), for $\lfloor w/2 \rfloor < k \leq \text{length}(V_{input}) - \lfloor w/2 \rfloor$.

$$X = V_{input}\left[k - \lfloor w/2 \rfloor : k + \lfloor w/2 \rfloor\right] \tag{3}$$

Fig. 2 depicts the pseudocode for the piecewise moving average filter, and the operations performed within each sliding window are discussed in the following subsections.

A. Outlier Removal

Search and removal of outliers are the first steps in pre-processing the rms voltage profile. Outliers are commonly present in real measurement data, mainly originated from inappropriate treatment of missing data. In the scope of this work, rms voltage values during instantaneous voltage variation events are also considered outliers. This assumption is made because these events do not create a long-term step change in the system rms voltage level.

The presence of outliers may hinder statistical properties of the original data, such as mean and standard deviation [17]. Outlier detection and removal are performed through the Hampel identifier, which is a robust and efficient outlier detector, and does not require prior knowledge of the data distribution [18]. According to this technique, the value $V_{input}[k]$ is considered an outlier if

$$\frac{|V_{input}[k] - median(X)|}{MAD(X)} \geqslant 3 \tag{4}$$

where MAD represents the median absolute deviation and it is calculated as $MAD(X) = median(|X - median(X)|)$. If the condition in (4) is satisfied, the outlier is removed and replaced by its expected value, i.e., $V_{input}[k] = median(X)$.

Fig. 3 illustrates the outlier detection process through the Hampel identifier for a simulated random signal with $w = 21$. Note that the minimum and maximum limits in this identifier follow the variation observed in the rms voltage signal (V_{input}). The final samples in the observation window present

Algorithm 1 Piecewise moving average filter

Inputs:

V_{input}: unfiltered rms voltage profile
w: length of the piecewise moving average filter
w_{median}: length of the final median filter

Outputs:

V_{rms}^{filt}: filtered rms voltage profile

for all k **do**
  $X \leftarrow V_{input}[k - \lfloor w/2 \rfloor : k + \lfloor w/2 \rfloor]$
  $V_{before} \leftarrow V_{input}[k - \lfloor w/2 \rfloor : k - 1]$
  $V_{after} \leftarrow V_{input}[k + 1 : k + \lfloor w/2 \rfloor]$
  $w_t \leftarrow \lfloor w/4 \rfloor$
  if $V_{input}[k]$ is an outlier **then** ▷ Hampel identifier
    $V_{input}[k] \leftarrow \text{median}(X)$
  end if
  while length$(V_{before}) > w_t$ **do**
    if $\mu_{V_{before}} = \mu_{V_{after}}$ **and** $var_{V_{before}} = var_{V_{after}}$ **then** ▷ Using two-sample t-test and F-test
      $V_{rms}^{filt}[k] = \text{mean}(X)$
      break
    else
      $V_{before} \leftarrow V_{before}[2 : end]$
      $V_{after} \leftarrow V_{after}[1 : end - 1]$
      $X \leftarrow [V_{before}, V_{input}[k], V_{after}]$
    end if
  end while
  if length$(V_{before}) = w_t$ **then**
    Compute $D(V_{before})$ and $D(V_{after})$
    $V_{select} \leftarrow \{V \in \{V_{before}, V_{after}\} | D(V)$ is min.$\}$
    $V_{rms}^{filt}[k] \leftarrow \text{mean}(V_{select})$
  end if
end for
Apply final median filter with length w_{median}

Fig. 2. Pseudocode for the piecewise moving average filter.

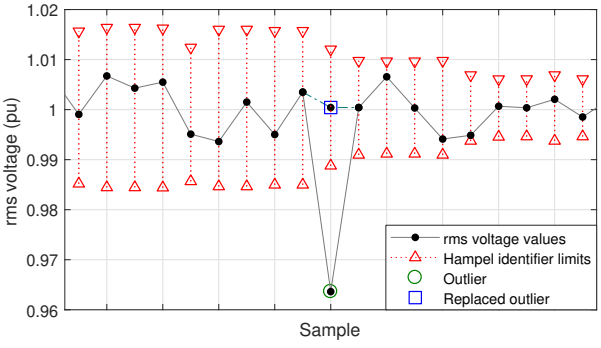

Fig. 3. Illustration of the Hampel identifier in detecting and removing outliers.

less fluctuations than the initial ones, resulting in a narrower range of values for non-outliers at the end of the signal. This behavior is caused by a reduction in the value of MAD.

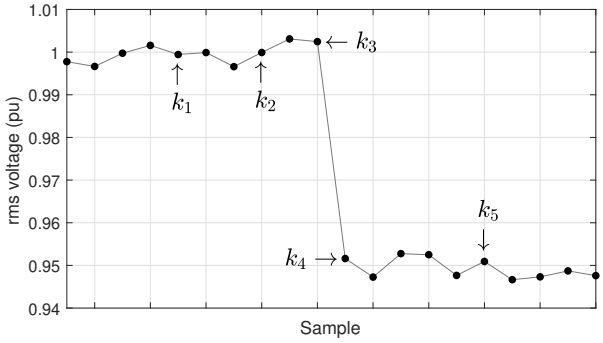

Fig. 4. Simulated random signal used to illustrate the application of the t-test and F-test during steady-state and rms voltage step change conditions.

TABLE I. TEST DECISION FOR THE NULL HYPOTHESES FOR TWO-SAMPLE T-TEST AND F-TEST FOR $w = 8$ SAMPLES

Index	Decision for the null hypothesis	
	t-test	F-test
$\boldsymbol{k_1, k_5}$	Accept	Accept
$\boldsymbol{k_2}$	Possibly reject	Possibly reject
$\boldsymbol{k_3, k_4}$	Reject	Accept

B. Detection of Possible rms Voltage Step Changes

The detection of an rms voltage step change at index k is based on rms voltage values immediately before and after index k. In order to perform this detection, the sliding window X is divided into 2 subsets: unfiltered rms values before and after index k, respectively, as represented in (5). The number of samples in each subset is at most half of the filter length.

$$\begin{aligned} V_{before} &= V_{input}[k - \lfloor w/2 \rfloor : k - 1] \\ V_{after} &= V_{input}[k + 1 : k + \lfloor w/2 \rfloor] \end{aligned} \tag{5}$$

These 2 subsets are compared through the two-sample t-test (mean equality) and F-test (variance equality). The null hypotheses are that both subsets have equal mean and variance, respectively. Both tests assume a normal distribution; in other words, the rms voltage profile is assumed to converge to a normal distribution if the number of samples is sufficiently large (central limit theorem). It will be shown in Subsection IV-A that this assumption holds mostly true.

The application of the two-sample tests is discussed through Fig. 4, which represents a random simulated signal with an rms voltage step change at k_3. The test decision for the null hypotheses for each selected index is shown in Table I, assuming a filter length $w = 8$ samples.

V_{before} and V_{after} are assumed to originate from the same distribution (i.e., no rms voltage step change occurred at instant k) if both means and variances are equal with the typical significance level of 5% [19]. In this case, both null hypotheses are not rejected, and the filtered rms value for the current iteration is defined as the average of the entire window, i.e., $V_{rms}^{filt}[k] = mean(X)$. This case corresponds to k_1 and k_5 in Fig. 4. This operation corresponds to an iteration of a moving average filter.

On the other hand, if at least one of the null hypotheses is rejected, the first element of V_{before} and the last element

of V_{after} are removed, and X is updated accordingly. The goal of this process is to obtain smaller subsets that do not contain an rms voltage step change, resulting in statistically equal means and variances. For example, both null hypotheses for k_1 would possibly be rejected if $w = 12$ in Fig. 4; however, they would be accepted if the last sample of V_{after} is removed. This process is repeated until one of the following conditions occurs:

1. Both means and variances are statistically equal. In this case, neither V_{before} nor V_{after} contain an rms voltage step change. Thus, $V_{rms}^{filt}[k] = mean(X)$.
2. The reduced subsets contain less than $w_t = \lfloor w/4 \rfloor$ samples. This value is adopted to prevent performing statistical tests on very short datasets, since V_{before} and V_{after} deviate from a normal distribution when their length decreases. When $w_t < \lfloor w/4 \rfloor$, a voltage step change may have occurred at index k, as it is discussed in the next subsection.

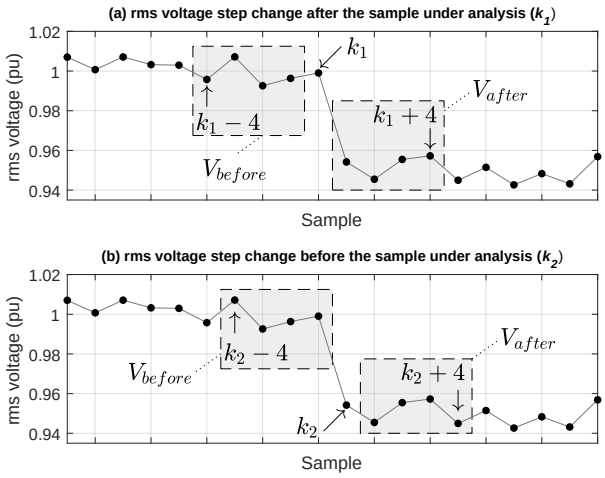

Fig. 5. Simulated random signal used to illustrate the determination of the rms voltage step change instant through the D factor.

C. Filtering rms Voltage Profile Nearby Step Changes

Once a possible rms voltage step change has been identified, it is necessary to determine if this shift occurred immediately before or after instant k. The D factor is defined as the sum of the absolute differences between $V_{input}[k]$ and all other elements in each subset, i.e.:

$$D(V^*) = \sum_{p=1}^{w_t} |V^*[p] - V_{input}[k]| \tag{6}$$

where V^* represents either V_{before} or V_{after}. This factor indicates how much $V_{input}[k]$ deviates from the other elements in each subset. The rms voltage step change occurred immediately before instant k if $D(V_{before}) > D(V_{after})$; otherwise, it occurred immediately after instant k. For example, Fig. 5a illustrates the case when the step change occurred immediately after k_1. It is possible to verify visually that $V_{input}[k_1 - 4 : k_1 - 1]$ have values similar to $V_{input}[k_1]$, while $V_{input}[k_1 + 1 : k_1 + 4]$ values are significantly lower. In this case, $D(V_{before}) = 0.0206$ and $D(V_{after}) = 0.1837$. Fig. 5b represents the opposite situation, where the rms voltage step change occurred immediately before k_2; in this case, $D(V_{before}) = 0.1783$ and $D(V_{after}) = 0.0233$.

The subset with the minimum D factor is selected as V_{select}, and $V_{rms}^{filt}[k] = mean(V_{select})$. Note that this operation corresponds to an iteration of a moving average filter. However, it does not affect the sharp edges of the rms voltage step change because V_{select} contains either values pre- or post-voltage step change, but not both.

The sliding window is moved 1 sample to the right and the process restarts to compute $V_{rms}[k+1]$, until the moving window reaches the end of the input vector. Lastly, a median filter is applied to reduce any remaining noise in the smoothed signal. The resulting filter is referred to as *piecewise moving average filter*.

D. Adaptive Limits for Step Change Detection

The inferior and superior limits for rms voltage step change detection are computed through the median absolute deviation approach. This is a robust method mostly unaffected by the presence of extreme values in the data set [18]. Its essence is to use s past values to determine the allowable range of values at the current instant r. It is determined that an rms voltage step change has occurred at the instant r if any of the conditions in (7) is satisfied, where $V_{adap} = V_{rms}^{filt}[r - s : r - 1]$.

$$\begin{aligned} V_{rms}^{filt}[r] &< median(V_{adap}) - 3 \times MAD(V_{adap}) \\ V_{rms}^{filt}[r] &> median(V_{adap}) + 3 \times MAD(V_{adap}) \end{aligned} \tag{7}$$

Note that this method is similar to the Hampel identifier described previously. However, the computation of adaptive limits uses exclusively past values to estimate the current expected value, while the Hampel identifier uses both past and future values to identify outliers in a time series.

IV. Validation and Applications

This section demonstrates the application of the piecewise moving average filter proposed in Section III, and compares its performance to the moving average and median filters. The test data consist in 28-minute continuous phase voltage measurements at the 25-kV substation transformer of a radial distribution system with multiple parallel feeders. The power quality monitor is installed at the feeder head, and its sampling frequency is 7.68 kHz. There are 9 rms voltage step changes during the measurement interval, resulting from 4 capacitor energizing and 5 capacitor de-energizing operations. Recurring capacitor switching operations in such a short time interval is not observed in the system under normal conditions. The dataset used in this section corresponds to test data, where the system operator manually overrode the capacitor switching control to obtain a desired sequence of switching events. The rms voltage profile is obtained by computing rms values over one-cycle sliding windows; multiple rms update rates, ranging from half-cycle to 1 second, were tested. Note: all the following plots have an rms update rate of 1 second, except the load energizing case (the update rate in this case is half-cycle).

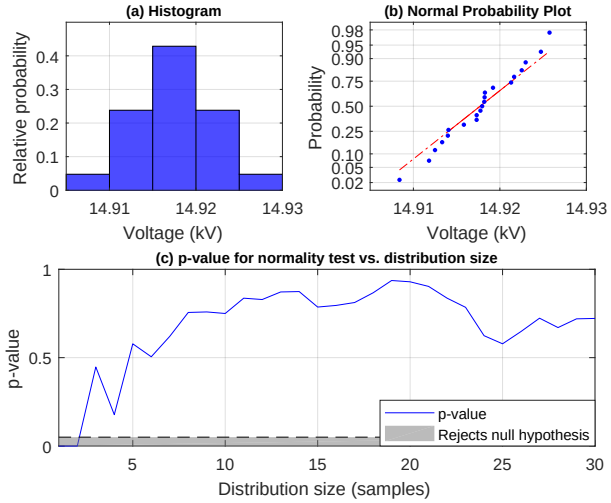

Fig. 6. Histogram and normal probability plot of an rms voltage profile with 21 samples and without an rms voltage step change, and p-values for multiple dataset sizes.

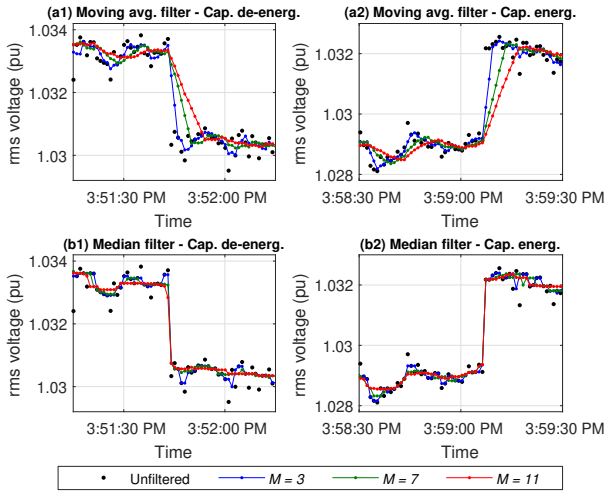

Fig. 7. RMS voltage profile filtered by (a1-a2) moving average and (b1-b2) median filters with lengths $M = 3$, 7, and 11 during capacitor de-energizing and energizing operations.

A. Assumption of Normality for the rms Voltage Profile

The statistical tests mentioned in Subsection III-B – two-sample t-test and F-test – are commonly applied for sets of data that follow a normal distribution. The method proposed in this paper assumes that any portions of the rms voltage profile without a step change converge to a normal distribution. Fig. 6 illustrates the histogram and normal probability plot for an rms voltage profile set composed of 21 samples. Visual inspection of Fig. 6a and 6b shows that the assumption made above is reasonable, as the histogram resembles a bell curve and the normal probability plot is a good approximation of a straight line. Moreover, the Shapiro-Wilk test [20] does not reject the null hypothesis that the samples come from a normally distributed population at a 5% significance level for all distributions with at least 3 samples. Note in Fig. 6c that longer datasets have higher p-values, i.e., they are closer to an ideal normal distribution, as stated by the central limit theorem. Nevertheless, the p-value may drop depending on the most recent rms voltage values added to the distribution, as observed for datasets with more than 20 samples.

B. Moving Average and Median Filters

Moving average and median filters are initially tested to illustrate their poor performance during rms voltage step changes. The rms voltage values at index k filtered through moving average and median filters with length M are computed as shown in (8a) and (8b), respectively.

$$V_{rms}^{avg}[k] = \frac{1}{M} \sum_{p=k-M+1}^{k} V_{input}[p] \tag{8a}$$

$$V_{rms}^{med}[k] = median(V_{input}[k-M+1:k]) \tag{8b}$$

Fig. 7(a1) and 7(a2) show the filtered rms voltage profile using moving average filters with lengths $M = 3$, 7, and 11 during capacitor de-energizing and energizing operations, respectively. While the steady-state rms voltage values become less noisy as the filter length increases, the step changes are also attenuated, i.e., blurred. In fact, a moving average filter with length M introduces $(M-1)$ intermediary points between the two voltage levels.

Median filters also have drawbacks in filtering the rms voltage profile. Fig. 7(b1) and 7(b2) represent the filtered rms voltage profile using median filters with lengths $M = 3$, 7, and 11 during capacitor de-energizing and energizing operations, respectively. Unlike the moving average filter, the median filter is able to retain the sharp edges during rms voltage step changes. However, these plots illustrate how the choice of an appropriate filter length is critical. With $M = 3$, the filter is not able to eliminate most of the noise in the rms voltage profile; in this case, the filtered voltage profile follows the trend of rapid fluctuations observed in the original signal. On the other hand, longer median filters are able to remove the noise, while potentially reducing the magnitude of the step change. For example, consider the case $M = 11$ in Fig. 7(b1), where the filtered rms voltage starts decreasing prior to the true rms voltage step change (this initial voltage reduction is 14.8% of the actual step change magnitude). In this case, even though the event is detected, its characterization is not accurate. Moreover, underdetection may occur for larger initial voltage reductions, as the filtered rms voltage profile would have one intermediary point between the two steady-state voltage levels, similar to moving average filters.

C. Piecewise Moving Average Filter

The rms voltage profile obtained by the proposed piecewise moving average filter is shown in Fig. 8a. The filter length, w, is chosen as 21; therefore, the minimum number of samples for performing the t-test and F-test is 5, as defined Section III. The median filter applied at the end of the smoothing process has length $w_{median} = 11$.

The detailed rms voltage profile during capacitor de-energizing and energizing, and steady-state operations are shown in Fig. 8b, 8c, and 8d, respectively. Note that the filtered output satisfies both requirements: removal of the rapid fluc-

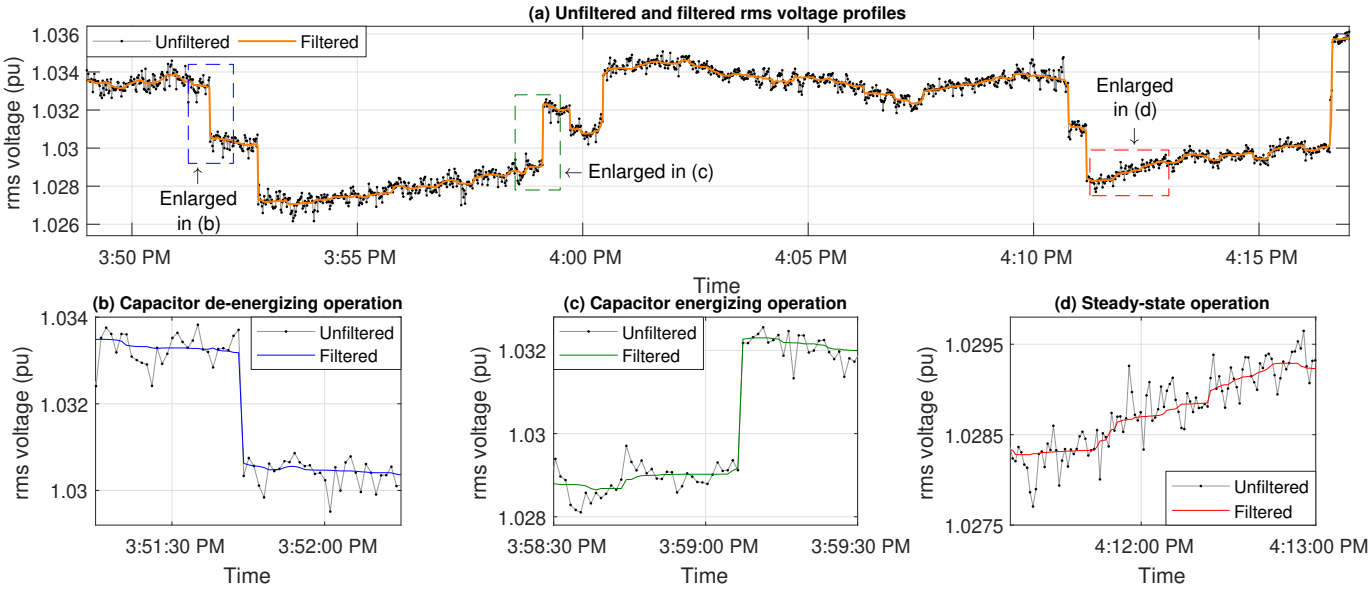

Fig. 8. RMS voltage profile filtered by the piecewise moving average filter with length $w = 21$ (a) for the entire monitoring period, during capacitor (b) de-energizing, (c) energizing, and (d) steady-state operations. The median filter has length $w_{median} = 11$.

tuations during steady-state, and preservation of sharp edges during rms voltage step changes, without affecting the step magnitude. In Fig. 8b, the filtered value immediately before the step change is lower than the original value; however, there is no reason to believe that the step change magnitude has been reduced in the filtered profile, as it follows the trend of unfiltered values.

D. Adaptive Limits for rms Voltage Step Change Identification

The inferior and superior limits for rms voltage step change detection are computed as described in Subsection III-D, adopting $s = 15$ samples. An rms voltage step change is detected whenever the rms voltage value lies outside the range defined by these limits. Fig. 9a shows rms voltage step changes corresponding to either a capacitor energizing (positive rms voltage variation) or de-energizing (negative rms voltage variation) operation.

Note that the inferior and superior limits are represented by a horizontal, straight line immediately after an rms voltage step change has been detected. As mentioned before, the rms voltage profile converges to a normal distribution with different mean after a step change; therefore, computation of these limits after the step change should not include the rms voltage values prior to the step change. In fact, consider that an rms voltage step change has been identified at index r, and these limits are computed using the previous s samples. Thus, the limit values for indices ranging from $(r + 1)$ to $(r + s)$ will be set equal to the limit values at index $(r + s + 1)$.

For comparison purposes, the proposed detection algorithm is tested with the unfiltered rms voltage profile. While the piecewise moving average filter contains 0 false-positive detections, using the unfiltered rms voltage profile resulted in 17 false-positive rms voltage step changes. The hollow orange squares in Fig. 9b, 9c, and 9d correspond to some of these overdetections.

Due to the drawbacks discussed previously, rms voltage step change detection is not accurate if the signal is filtered using either a moving average filter (misses step changes because of the smoothed edges) or median filter (overdetects step changes because the filtered signal tends to follow the trend of the rapid voltage fluctuations). The performance of each filter is quantified through its true positive (TP) and false positive (FP) values. Ideally, TP should be 9 (total number of rms voltage step changes in the dataset under analysis; the rms voltage increase near the end of the measurement interval corresponds to two capacitor energizing operations and it is discussed in details in Subsection IV-E) and FP sould be 0. The results are presented in Table II; note that both moving average and median filters perform poorly, regardless of the rms update rate. The filter length for the piecewise moving average filter corresponds to the length of the median filter applied at the end of the smoothing process, w_{median} (see Subsection III-C); note that this value has little influence on the output profile.

Although the median filter with length $M = 11$ seems a good option for rms voltage step change detection, it may misrepresent the step change magnitude in some cases, as shown in Fig. 7(b1). Moreover, it is not possible to determine the minimum length of a median filter that reduces false positive detections in all cases due to the randomness of the rapid voltage fluctuations. For example, Fig. 10 represents the rms voltage profile filtered by median ($M = 3$, 7, and 11) and piecewise moving average filters for a portion of the signal without any rms voltage step changes. The false positive detections for the median filter with $M = 3$ and 7 occurred shortly before 4:10 PM, where the filtered rms values are slightly higher than the superior limit. Increasing the filter length to $M = 11$ eliminated this false positive detection; however, the filtered profile in this case is still significantly affected by the rapid voltage fluctuations, and its performance cannot be generalized to all datasets. On the other hand, the

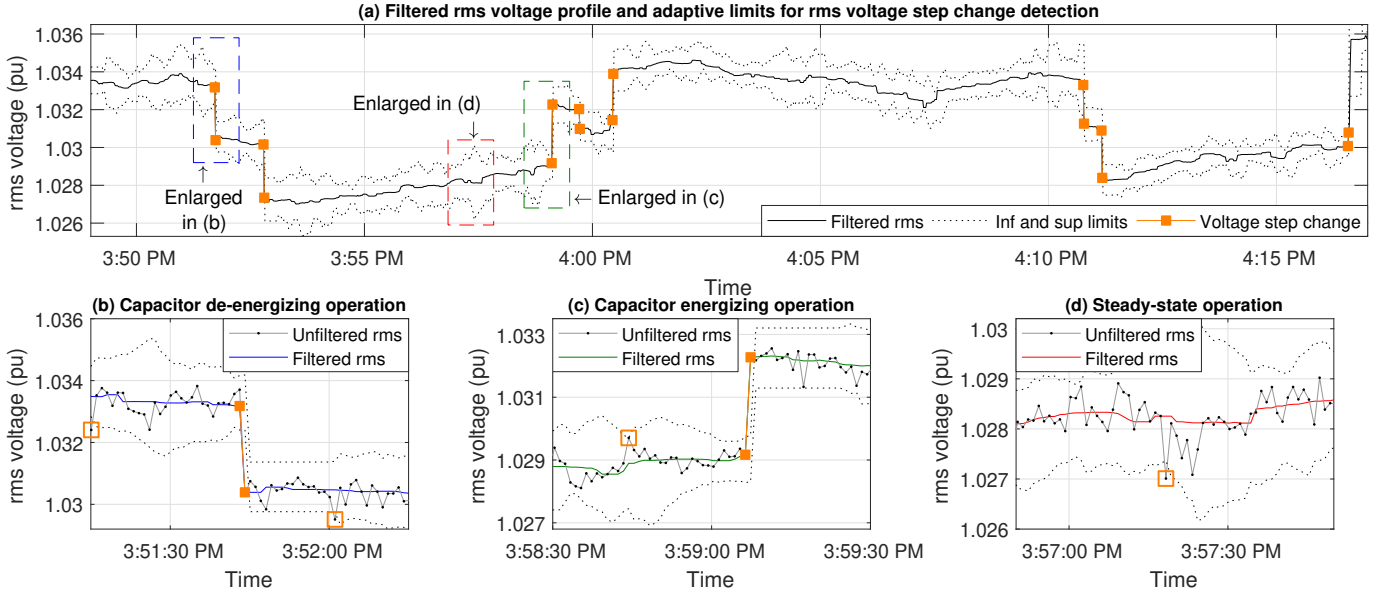

Fig. 9. Detection of rms voltage step changes (a) for the entire monitoring period, during capacitor (b) de-energizing, (c) energizing, and (d) steady-state operations. The solid and hollow orange squares represent the step changes detected by the proposed method using filtered and unfiltered profiles, respectively.

TABLE II. NUMBER OF TRUE POSITIVE (TP) AND FALSE POSITIVE (FP) RMS VOLTAGE STEP CHANGE DETECTIONS FOR EACH FILTER

Filter type	rms update rate (s)	Filter length 3 TP	3 FP	7 TP	7 FP	11 TP	11 FP
Moving average	1/120*	8	2	0	0	0	0
	0.2	8	1	1	0	1	0
	0.4	7	0	0	0	0	0
	0.6	5	0	0	0	0	0
	0.8	5	0	0	0	0	0
	1	3	0	0	0	0	0
Median	1/120*	8	1	8	1	7	1
	0.2	8	8	8	2	8	1
	0.4	8	5	8	1	8	0
	0.6	8	5	8	0	8	0
	0.8	8	2	8	0	7	0
	1	8	1	8	1	8	0
Piecewise moving average	1/120*	9	0	9	0	9	0
	0.2	9	0	9	0	9	0
	0.4	8	0	8	0	8	0
	0.6	8	0	8	0	8	0
	0.8	8	0	8	0	8	0
	1	8	0	8	0	8	0

* Update rate is half-cycle, as in the $U_{rms(1/2)}$ definition

absence of rms voltage step changes in this portion of the signal indicates that the null hypothesis of both t-test and F-test are not rejected; and, therefore, the proposed filter uses average operations to obtain the output profile. The resulting profile is smooth and unaffected by the rapid voltage fluctuations.

E. Limitations

In the previous examples, the interval between consecutive rms computations, Δt_{rms}, is 1 second. At the end of the measuring interval (between 4:16:30 PM and 4:16:40 PM), there are 2 successive capacitor bank energizing operations less than 3 seconds apart from each other. Therefore, when analyzing the first energizing operation, V_{after} contains rms values computed after the second one. This fact may prevent the correct rms voltage step change identification, as represented in Fig. 11a. On the other hand, Fig. 11b shows the rms voltage profile for $\Delta t_{rms} = 0.2$ second; in this case, both rms voltage step changes are correctly identified.

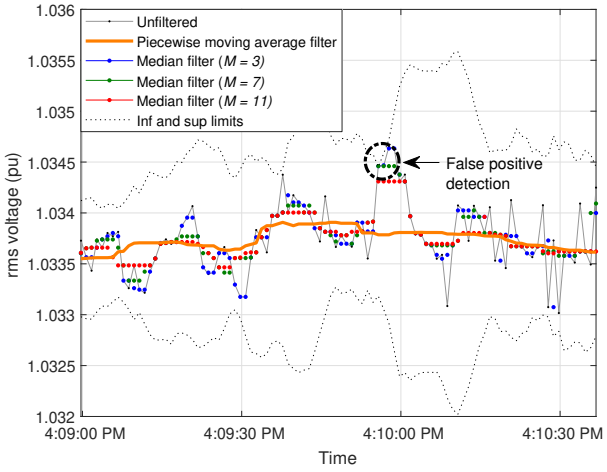

Fig. 10. RMS voltage profile filtered by median (M = 3, 7, and 11) and piecewise moving average filters during steady-state operation.

The identification of successive rms voltage step changes is possible if the filter time resolution, $r_t = \lfloor w/2 \rfloor \times \Delta t_{rms}$, is smaller than the minimum interval between successive step changes. In fact, the second capacitor energizing is detected if $r_t \leq 3$ (i.e., $\Delta t_{rms} \leq 0.3$ second), which is confirmed in Table II. The choice for Δt_{rms} represents a compromise between computational effort and robustness, as larger values decrease

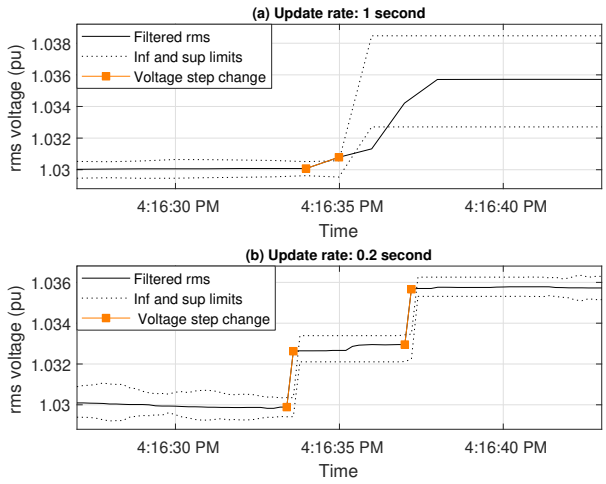

Fig. 11. RMS voltage profile filtered by the piecewise moving average filter with length $w = 21$ during successive capacitor energizing operations. The rms voltage update rates are (a) 1 s and (b) 0.2 s.

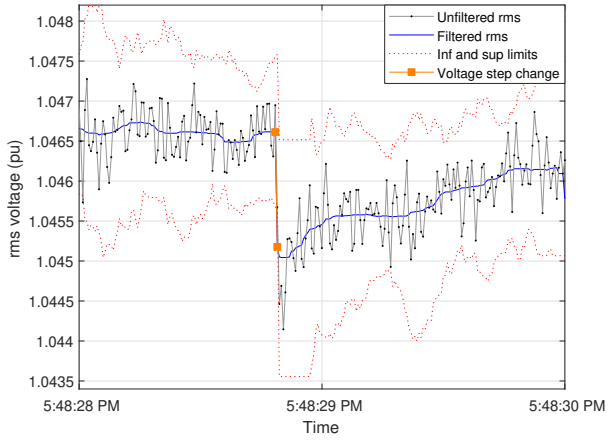

Fig. 12. RMS voltage profile filtered by the piecewise moving average filter with length $w = 21$ during a load energizing.

the computational effort but allows for the underdetection of successive rms voltage step changes, and vice-versa.

F. Load Energizing Application

As a final case, Fig. 12 represents the rms voltage profile during a load energizing (the corresponding increase in active power flow is about 18 kW). Detecting the rms voltage step change caused by this load energizing is challenging if the rms voltage profile is unfiltered. In fact, note that the valleys before the energizing and peaks after the energizing have similar values. On the other hand, this step change was successfully identified on the filtered rms voltage profile using the adaptive limits and the piecewise moving average filter.

V. Conclusion

The piecewise moving average filter proposed in this paper is robust in attenuating the rapid fluctuations observed in rms voltage profiles, while preserving the sharp edges during rms voltage step changes. This approach reduces the time required to identify power quality switching events in instantaneous voltage waveforms. A detailed search is needed only when an rms voltage step change has been detected. The rms update rate has small influence on the detection of these step changes, as long as the interval between consecutive events is larger than the filter time resolution. In general, switching events create a sustained change in the voltage level, which persists until a new operation occurs; therefore an rms update rate of 1 second is suitable. Switching of large loads is an exception, as the voltage recovers to the pre-event value in few seconds; in this case, the rms voltage profile must have a higher time resolution (for example, rms values updated every half-cycle, as in the $U_{rms(1/2)}$ definition). A lower rms voltage time resolution may be chosen when it is not required to detect the switching of large loads. Although the proposed method is illustrated for the identification of capacitor switching events, it is applicable to any event that creates an rms voltage step change.

References

[1] W. Xu, "Experiences on using gapless waveform data and synchronized harmonic phasors," Panel Session in IEEE Power and Energy Society General Meeting, Tech. Rep., 2015.
[2] L. Silva, E. Kapisch, C. Martins, L. Filho, A. Cerqueira, C. Duque, and P. Ribeiro, "Gapless power-quality disturbance recorder," *IEEE Trans. Power Del.*, vol. 32, no. 2, pp. 862–871, Apr. 2017.
[3] B. Li, Y. Jing, and W. Xu, "A generic waveform abnormality detection method for utility equipment condition monitoring," *IEEE Trans. Power Del.*, vol. 32, no. 1, pp. 162–171, Feb. 2017.
[4] S. Santoso, E. J. Powers, W. M. Grady, and A. C. Parsons, "Power quality disturbance waveform recognition using wavelet-based neural classifier - part 1: Theoretical foundation," *IEEE Trans. Power Del.*, vol. 15, no. 1, pp. 222–228, Jan. 2000.
[5] A. F. Bastos and S. Santoso, "Identifying switched capacitor relative locations and energizing operations," in *Proc. IEEE Power and Energy Society General Meeting*, 2016.
[6] M. Bollen and I. Gu, *Signal Processing of Power Quality Disturbances*. Hoboken, NJ: Wiley, 2006.
[7] *IEC Electromagnetic Compatibility: Testing and measurements techniques - Power quality measurement methods*, IEC 61000-4-30, 2015.
[8] *IEEE Guide for Voltage Sag Indices*, IEEE Std. 1564-2014, March 2014.
[9] T. A. Short, *Electric Power Distribution Handbook*. CRC Press, FL: Boca Raton, 2003.
[10] *IEEE Guide for Application of Shunt Power Capacitors*, IEEE Std. 1036-2010, January 2010.
[11] A. Salunkhe and S. Jagtap, "Robust feature-based digital video stabilization," *Int. J. Adv. Res. Electron. Commun. Eng.*, vol. 4, no. 8, pp. 2163–2167, Aug. 2015.
[12] S. Smith, *The Scientist and Engineer Guide to Digital Signal Processing*. San Diego: California Tech. Pub., 1997.
[13] G. Arce, *Nonlinear Signal Processing*. Hoboken, NJ: Wiley, 2005.
[14] W. Pratt, *Digital Image Processing*, 4th ed. Hoboken, NJ: Wiley, 2007.
[15] *IEEE Recommended Practice and Requirements for Harmonic Control in Electric Power Systems*, IEEE Std. 519-2014, March 2014.
[16] S. Santoso, *Fundamentals of Electric Power Quality*. Scotts Valley, CA: CreateSpace, 2012.
[17] R. Pearson, "Outliers in process modeling and identification," *IEEE Trans. Control Syst. Technol.*, vol. 10, no. 1, pp. 55–63, Jan. 2002.
[18] C. Leys, O. Klein, P. Bernard, and L. Licata, "Detecting outliers: Do not use standard deviation around the mean, use absolute deviation around the median," *J. Exp. Soc. Psychol.*, vol. 49, no. 4, pp. 746–766, 2013.
[19] *NIST/SEMATECH e-Handbook of Statistical Methods*. National Institute of Standards and Technology, 2012. [Online]. Available: http://www.itl.nist.gov/div898/handbook/
[20] A. Ghasemi and S. Zahediasl, "Normality tests for statistical analysis: A guide for non-statisticians," *Int. J. Endocrinol. Metab.*, vol. 10, no. 2, pp. 486–489, Apr. 2012.

Alvaro Furlani Bastos (S'15) received his B.Sc. degree in Electrical Engineering from the Federal University of Viçosa, Brazil, in 2014, and his M.Sc. degree in Electrical and Computer Engineering from The University of Texas at Austin in 2015, where he is currently pursuing his Ph.D. degree. His research interests include power quality and data analytics.

Keng-Weng Lao (S'09-M'17) was born in Macau, China, in 1987. He received the B.Sc., M.Sc., and Ph.D. degrees in Electrical and Electronics Engineering from the Faculty of Science and Technology, University of Macau, Macao, in 2009, 2011, and 2016, respectively. He is currently a lecturer in the Department of Electrical and Computer Engineering at University of Macau. He is now also as a research scholar in the Department of Electrical and Computer Engineering at The University of Texas at Austin. His research interests include power quality compensation, renewable energy integration, energy saving and power system.

Dr. Lao was the recipient of the Macao Science and Technology Development Fund-Postgraduate Award for Ph.D. Student 2016. He was also the first runner-up of the Challenge Cup National Inter-varsity Science and Technology Competition, and Championship of the Postgraduate Section in the IET Young Professionals Exhibition and Competition in China and Hong Kong, respectively, in 2013. He also received the Champion Award of the Schneider Electric Energy Efficiency Cup in Hong Kong in 2010. He was secretary and publication chair of the conference IEEE TENCON 2015.

Grazia Todeschini (SM'14) received her B.Sc. and M.Sc. in Electrical Engineering from the Politecnico di Milano, Italy, and her Ph.D. in Electrical and Computer Engineering from Worcester Polytechnic Institute in Massachusetts. She was Senior Consultant with EnerNex in Knoxville from 2010 to 2013, and Senior Power Studies Engineer with General Electric in Philadelphia from 2013 to 2016. She became Senior Lecturer at Swansea University, UK, in 2016. Her research interests include power quality, renewable energy integration, and power system analysis.

Surya Santoso (F'15) earned his B.S. degree from Satya Wacana Christian University, Salatiga, Indonesia, in 1992, and M.S.E. and Ph.D. degrees in Electrical and Computer Engineering from The University of Texas at Austin, in 1994 and 1996, respectively. He was a Senior Power Systems and Consulting Engineer with Electrotek Concepts, Knoxville, TN, USA, from 1997 to 2003. He joined the faculty of The University of Texas at Austin in 2003 and is currently Professor of Electrical and Computer Engineering. His research interests include power quality, power systems, and renewable energy integration in transmission and distribution systems. He is co-author of *Electrical Power Systems Quality* (3^{rd} edition), sole author of *Fundamentals of Electric Power Quality*, and editor of *Handbook of Electric Power Calculations* (4^{th} edition) and *Standard Handbook for Electrical Engineers* (17^{th} edition). He is an IEEE Fellow.